XLI CILAMCE
XLI Ibero-Latin American Congress on Computational Methods in Engineering
16-19 November, 2020 FOZ DO IGUAÇU PARANÁ - BRAZIL

A superconvergent piezoelectric beam finite element

Adriano L. Carvalho Neto, Regiane P. Barros, Eliseu Lucena Neto, Francisco A. C. Monteiro

Divisão de Engenharia Civil-Aeronáutica, Instituto Tecnológico de Aeronáutica
Praça Marechal Eduardo Gomes, 50, 12228-900, SP/São José dos Campos, Brazil
adricarv@ita.br, regianefp@hotmail.com, eliseu@ita.br, facm@ita.br

Abstract. A piezoelectric beam finite element is proposed, where the displacement is assumed to vary in accordance with the Timoshenko assumption and the electric potential has linear variation through each piezoelectric layer thickness. The solution of the homogeneous form of the linear differential equations which describe the behavior of the piezoelectric Timoshenko beam is used as interpolation functions to develop a 2-node finite element for planar frames. According to the adopted procedure the element has the following properties: (a) it has the same degrees of freedom as its purely mechanical counterpart; (b) it is free of shear locking; (c) it is superconvergent, i.e. the computed nodal values are exact with respect to the element formulation regardless the applied loading pattern. In the solution of the numerical examples, the efficiency of the developed finite element is illustrated showing that few elements are adequate to precisely capture the static response for both mechanical and electrical variables.

Keywords: superconvergence, piezoelectric beam, finite element.

1 Introduction

Smart materials are those that exhibit some type of coupling between different physical domains and may have their characteristics modified by controlled changes of state variables that characterize the mechanical, electrical, thermal and chemical domains, for example. Thus, piezoelectric materials are classified as smart because they exhibit coupling between the mechanical and electrical domains [1]. Piezoelectrics, available in the form of thin sheets of ceramic or polymer, are the most popular and practical smart materials due to their coupled electromechanical properties, that make them suitable for use as distributed sensors and actuators to control structural response. In the sensor application, strains can be determined from measurements of induced electric potential (direct piezoelectric effect), whereas in actuator applications strains can be controlled through the input of appropriate electric potential (converse piezoelectric effect). The technology of self-monitoring and self-controlling smart structures, by integrating distributed piezoelectric sensors and actuators, provides the possibility for the development of light-weight and rigid structures.

There are a number of beam theories that are used to represent the kinematics of deformation of one dimensional piezoelectric finite element [2]. The simplest beam theory is the Euler-Bernoulli beam theory, which assumptions amount to neglecting both transverse shear and transverse normal effects, i.e. deformation is due entirely to bending and inplane stretching [3-5]. It can be effectively used for the analysis of thin and slender piezoelectric smart beams. The next one in the hierarchy of beam theories is the Timoshenko beam theory, which relaxes the normality assumption of the Euler-Bernoulli beam theory and includes a constant state of transverse shear strain with respect to the thickness coordinate. Since the transverse shear strain in the Timoshenko beam theory is represented as a constant through the beam thickness, a shear correction factor is introduced to calculate the transverse shear force that would be equal in magnitude to the actual shear force. Timoshenko-based beam finite elements differ from each other in the choice of interpolation functions used for the transverse displacement and rotation or in the weak form used to develop the finite element model [6]. They are widely used in the literature for the analysis of piezoelectric smart structures [7-11].

In solving differential equations by the finite element method, it has been found that the rate of conver-

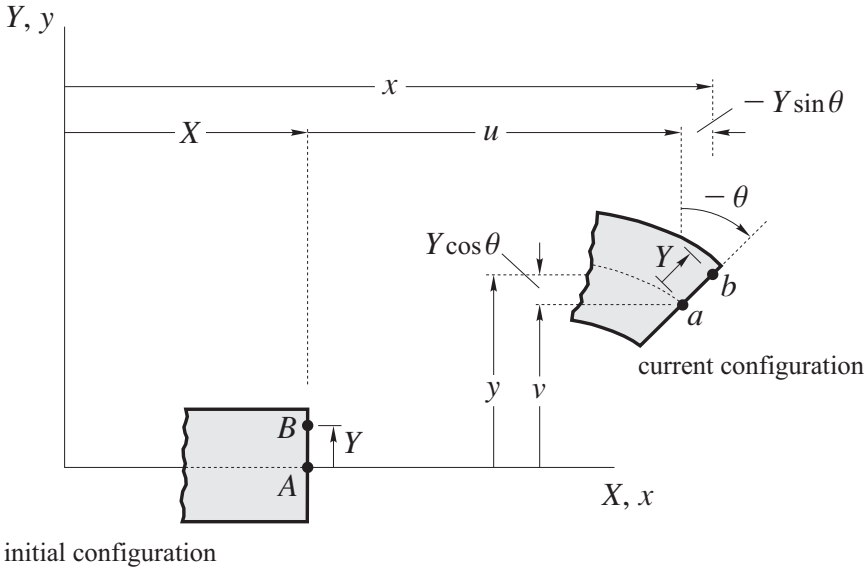

Figure 1. Timoshenko beam kinematics

gence of finite element solutions at some exceptional points of a domain exceeds the optimal global rate. This phenomenon has come to be known as *superconvergence* [12], which first proof is usually attributed to Douglas and Dupont [13]. Superconvergence is of considerable interest not only from a theoretical but also from a practical viewpoint. There are several important applications of superconvergence results. For instance, a nodal superconvergence of finite element approximations is used for creating adaptive mesh refinements and a posteriori error estimates.

We developed in this paper a superconvergent piezoelectric beam finite element for plane frames. A linear element is proposed, whose displacement varies according to Timoshenko assumption and the electric potential has linear variation along with the thickness of each piezoelectric layer. The interpolation functions of the element are identified from the general solution of the homogeneous part of the system of equations that describes the linear problem. Such a feature makes the element to be superconvergent, i.e. nodal values are exact with respect to the element formulation regardless the loading pattern. In the solution of the numerical examples, it is shown that few elements are adequate to precisely capture the nodal static response for both mechanical and electrical variables. Nothing is yet known about the accuracy of the electrical quantities obtained by such a type of element. To prove a nodal superconvergence for the difference of electric potential in the piezoelectric layers seems to be an open problem for the time being.

2 Fundamentals

A straight beam with attached piezoelectric layers is considered. The displacement field varies in accordance with the Timoshenko assumption while the electric potential is assumed linear through each piezoelectric layer thickness.

2.1 Displacement, strain, electric potential and electric field

Suppose that a point B of the beam shown in Fig. 1 in the initial configuration moves to the point b in the current configuration with motion lying in the XY plane. Under the Timoshenko assumption [14], the cross-section is taken to be infinitely rigid in its own plane, remaining plane but not necessarily perpendicular to the beam axis during the motion. For small rotations, the displacement field of the beam reads

$$u_x(X,Y) = u(X) + Y\beta(X) \qquad u_y(X,Y) = v(X) \tag{1}$$

where the displacement u and v refer to the point A on the beam axis, which moves to the point a, and β is the cross-section rotation. Assuming that the components of the strain tensor are small, its non-null entries read

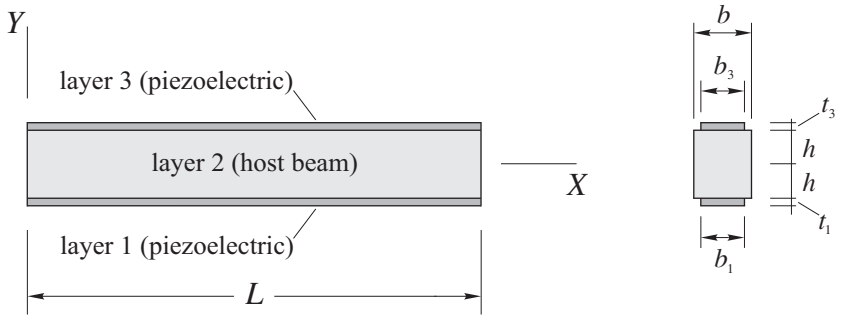

Figure 2. Beam with bottom and top piezoelectric layers

$$\epsilon_x(X,Y) = \epsilon_0(X) + Y\kappa(X) \qquad \gamma_{xy}(X,Y) = \gamma(X) \tag{2}$$

with

$$\epsilon_0(X) = u' \qquad \kappa(X) = \beta' \qquad \gamma(X) = v' + \beta. \tag{3}$$

A prime indicates differentiation with respect to X.

Figure 2 shows a host beam of length L, having a rectangular cross section of width b and thickness $2h$, with two piezoelectric layers bonded on its bottom and top surfaces. The lower layer has width b_1 and thickness t_1, and the upper layer has width b_3 and thickness t_3. Because the electric field vector $\boldsymbol{E}$ is irrotational one has

$$\boldsymbol{E} = \lfloor E_x \quad E_y \quad E_z \rfloor^T = -\left\lfloor \frac{\partial \phi}{\partial X} \quad \frac{\partial \phi}{\partial Y} \quad \frac{\partial \phi}{\partial Z} \right\rfloor^T \tag{4}$$

where ϕ is a scalar function known as electric potential. Because the motion of the beam lies in the XY plane one specifies $E_z = 0$. Indeed, assuming that the gradient of electric potential through the thickness of a piezoelectric layer is the only to be considered [15-18] then $E_x \approx 0$. Since the electric potential varies linearly through the thickness of a piezoelectric layer k [19], between the values ϕ_k at the bottom ($Y = Y_k$) and ϕ_{k+1} at the top ($Y = Y_k + t_k$) of the layer, then

$$\phi(X,Y) = \left(1 - \frac{Y - Y_k}{t_k}\right)\phi_k(X) + \frac{Y - Y_k}{t_k}\phi_{k+1}(X) \qquad k = 1, 3. \tag{5}$$

The nonzero component of $\boldsymbol{E}$ reduces to

$$E_y = -\frac{\bar{\phi}_k}{t_k} \tag{6}$$

in which $\bar{\phi}_k = \phi_{k+1} - \phi_k$ is the voltage (difference of electric potential) in the piezoelectric layer k.

2.2 Principle of virtual displacements

The principle of virtual displacements for the piezoelectric beam, shown schematically in Fig. 3, takes the form [20]:

$$-\int_0^L (N\delta\epsilon_0 + M\delta\kappa + Q\delta\gamma + L_1\delta\bar{\phi}_1 + L_3\delta\bar{\phi}_3)dX + \int_0^L \left(q_x\delta u + q_y\delta v\right)dX$$
$$+ \sum_{i=1}^{2} \left(F_{xi}\delta u_i + F_{yi}\delta v_i + M_{zi}\delta\theta_i\right) = 0 \tag{7}$$

with

$$N = \int_A \sigma_x dA \qquad M = \int_A \sigma_x y dA \qquad Q = \int_A \sigma_{xy} dA$$

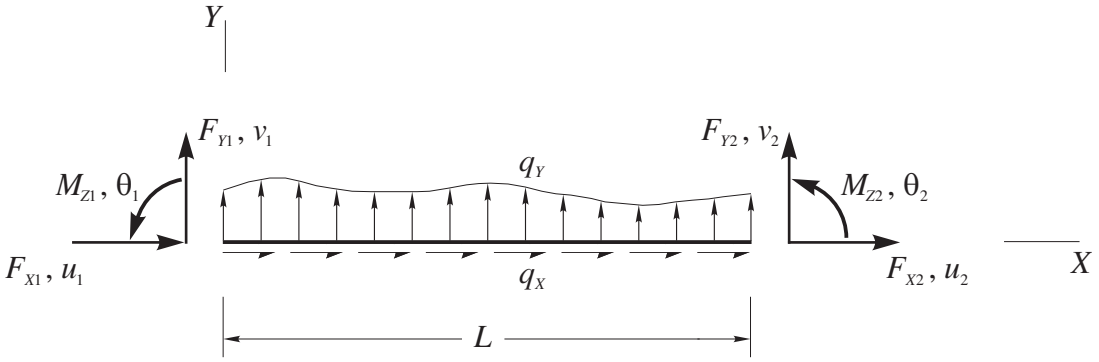

Figure 3. Free-body diagram of a piezoelectric beam showing all the applied loads and the end displacements

$$L_1 = \frac{b_1}{t_1}\int_{-h-t_1}^{-h} D_y dY \qquad L_3 = \frac{b_3}{t_3}\int_{h}^{h+t_3} D_y dY \tag{8}$$

where σ_x and σ_{xy} are the normal and transverse shear stress; D_y is the transverse electric displacement; q_x and q_y are the distributed axial and transverse forces (force per unit length); F_{xi}, F_{yi} and M_{zi} are the end loads; u_i, v_i and θ_i are the end displacements; A is the piezoelectric beam cross-section area.

Performing integration by parts in Eq. (7), taking into account Eq. (3), and then applying the fundamental lemma of variational calculus [21] yields the governing equations

$$N' = -q_x \qquad Q' = -q_y \qquad M' - Q = 0 \qquad L_1 = 0 \qquad L_3 = 0 \tag{9}$$

in the problem domain, $0 < X < L$. The first three equations represent the static equilibrium statement, while the last two equations are the application of Gauss law to the piezoelectric layers. The solution of Eq. (9) should satisfy the prescribed values of

$$\begin{aligned} &u_1 = \bar{u}_1 \text{ or } N = -F_{x1} \qquad v_1 = \bar{v}_1 \text{ or } Q = -F_{y1} \qquad \theta_1 = \bar{\theta}_1 \text{ or } M = M_{z1} \quad : X = 0 \\ &u_2 = \bar{u}_2 \text{ or } N = F_{x2} \qquad v_2 = \bar{v}_2 \text{ or } Q = F_{y2} \qquad \theta_2 = \bar{\theta}_2 \text{ or } M = -M_{z2} \quad : X = L \end{aligned} \tag{10}$$

where the quantities $\bar{u}_i$, $\bar{v}_i$ and $\bar{\theta}_i$ denote known values of u_i, v_i and θ_i.

2.3 Constitutive relations

Let an extension mode piezoelectric with polarization oriented in the positive Y- axis and remaining material principal directions aligned with the X- axis. According to the beam theory, the constitutive relations reduces to the simple form

$$\begin{Bmatrix} \sigma_x \\ \sigma_{xy} \\ D_y \end{Bmatrix} = \begin{bmatrix} \tilde{Q}_{11} & 0 & \tilde{e}_{31} \\ & KC_{55} & 0 \\ \text{sym.} & & -\tilde{\xi}_3 \end{bmatrix} \begin{Bmatrix} \epsilon_x \\ \gamma_{xy} \\ -E_y \end{Bmatrix} \tag{11}$$

where K is the shear correction factor [22, 23].

Following Butz et al. [24], Khdeir et al. [25], Elshafei et al. [26] and Sulbhewar and Raveendranath [27], the coefficients $\tilde{Q}_{11}$, $\tilde{e}_{31}$ and $\tilde{\xi}_3$are defined by

$$\tilde{Q}_{11} = Q_{11} - \frac{Q_{12}^2}{Q_{22}} \qquad \tilde{e}_{31} = \bar{e}_{31} - \frac{Q_{12}\bar{e}_{32}}{Q_{22}} \qquad \tilde{\xi}_3 = \bar{\xi}_3 + \frac{\bar{e}_{32}^2}{Q_{22}} \tag{12}$$

with

$$Q_{ij} = C_{ij} - \frac{C_{i3}C_{j3}}{C_{33}} \qquad \bar{e}_{3i} = e_{3i} - \frac{C_{i3}e_{33}}{C_{33}} \qquad \bar{\xi}_3 = \xi_3 + \frac{e_{33}^2}{C_{33}} \tag{13}$$

where C_{ij}, e_{ij} and ξ_i are the elastic, piezoelectric and dielectric coefficients [28].

Substitution of Eq. (2), Eq. (6) and Eq. (11) into Eq. (8) gives

$$\begin{Bmatrix} N \\ M \\ Q \\ L_1 \\ L_3 \end{Bmatrix} = \begin{bmatrix} A_{11} & A_{12} & 0 & A_{14} & A_{15} \\ & A_{22} & 0 & A_{24} & A_{25} \\ & & A_{33} & 0 & 0 \\ & \text{sym.} & & A_{44} & 0 \\ & & & & A_{55} \end{bmatrix} \begin{Bmatrix} \epsilon_0 \\ \kappa \\ \gamma \\ \bar{\phi}_1 \\ \bar{\phi}_3 \end{Bmatrix} \tag{14}$$

with

$$\begin{aligned} &A_{11} = \tilde{Q}_{111}A_1 + \tilde{Q}_{11b}A_b + \tilde{Q}_{113}A_3 \qquad A_{12} = \tilde{Q}_{111}A_1\left(\frac{t_1}{2}+h\right) - \tilde{Q}_{113}A_3\left(\frac{t_3}{2}+h\right) \\ &A_{14} = \tilde{e}_{311}\frac{A_1}{t_1} \qquad A_{15} = \tilde{e}_{313}\frac{A_3}{t_3} \\ &A_{22} = \tilde{Q}_{111}A_1\left(\frac{t_1^2}{3}+ht_1+h^2\right) + \frac{1}{3}\tilde{Q}_{11b}A_bh^2 + \tilde{Q}_{113}A_3\left(\frac{t_3^2}{3}+ht_3+h^2\right) \\ &A_{24} = \tilde{e}_{311}\frac{A_1}{t_1}\left(\frac{t_1}{2}+h\right) \qquad A_{25} = -\tilde{e}_{313}\frac{A_3}{t_3}\left(\frac{t_3}{2}+h\right) \\ &A_{33} = K(C_{551}A_1 + C_{55b}A_b + C_{553}A_3) \qquad A_{44} = -\tilde{\xi}_{31}\frac{A_1}{t_1^2} \qquad A_{55} = -\tilde{\xi}_{33}\frac{A_3}{t_3^2}. \end{aligned} \tag{15}$$

Here $\tilde{Q}_{111}$ and A_1 refer to the coefficient $\tilde{Q}_{11}$ and the cross-section area of the bottom piezoelectric layer; $\tilde{Q}_{11b}$ and A_b refer to the coefficient $\tilde{Q}_{11}$ and the cross-section area of the host beam; and so on.

3 Finite element model

Introducing the constant $C_i = 0$ or $C_i = 1$ in order to identify the piezoelectric layer i as actuator or sensor, respectively, the expression Eq. (7) is rewritten for a piezoelectric beam finite element of length L_e, in view of the strain-displacement equations Eq. (3) and the constitutive relations for N and M in Eq. (14), as

$$\begin{aligned} &-\int_0^{L_e}\left[N_\phi\delta u' + Q\delta(v'+\beta) + M_\phi\delta\beta' + C_1L_1\delta\bar{\phi}_1 + C_3L_3\delta\bar{\phi}_3\right]dX + \int_0^{L_e}\left[q_x\delta u + q_y\delta v\right. \\ &\left.-\phi_u\delta u' - \phi_\beta\delta(v'+\beta)\right]dX + \sum_{i=1}^{2}\left(F_{xi}\delta u_i + F_{yi}\delta v_i + M_{zi}\delta\theta_i\right) = 0 \end{aligned} \tag{16}$$

with

$$\begin{aligned} &N_\phi = A_{11}u' + A_{12}\beta' + C_1A_{14}\bar{\phi}_1 + C_3A_{15}\bar{\phi}_3 \qquad \phi_u = (1-C_1)A_{14}\bar{\phi}_1 + (1-C_3)A_{15}\bar{\phi}_3 \\ &M_\phi = A_{12}u' + A_{22}\beta' + C_1A_{24}\bar{\phi}_1 + C_3A_{25}\bar{\phi}_3 \qquad \phi_\beta = (1-C_1)A_{24}\bar{\phi}_1 + (1-C_3)A_{25}\bar{\phi}_3. \end{aligned} \tag{17}$$

The weak form Eq. (16) is associated with the following set of ordinary differential equations

$$N_\phi' = -q_x - \phi_u \qquad Q' = -q_y \qquad M_\phi' - Q = -\phi_\beta \qquad C_1L_1 = 0 \qquad C_3L_3 = 0 \tag{18}$$

in the element domain, $0 < X < L_e$, subjected to the boundary conditions Eq. (10). There are a few things worth mentioning about these equations: (a) when $C_1 = C_3 = 0$, the set reduces to the equilibrium equations; (b) a piezoelectric layer in actuation mode ($C_i = 0$) induces a uniform distributed axial load ϕ_u as, also as, a distributed moment load ϕ_β along the element length; (c) a piezoelectric layer in sensing mode ($C_i = 1$) introduces a linear dependency in the solution space; (d) the unknown voltages can be condensed out by substituting the equations related with the Gauss law into the equilibrium ones, enabling the solution space to be set only in terms of the mechanical unknowns.

Recall that the classical Euler-Bernoulli beam element gives exact nodal values because the element is based on the exact polynomial solution of the homogeneous problem. Analogously, one can develop a specialized piezoelectric beam element based on the exact solution of the homogeneous form of Eq. (18). A

priori this implies that the values of the primary variables u, v, β, $\bar{\phi}_1$, and $\bar{\phi}_3$ at the nodes are exact independent of the load distribution because the finite element approximation space is the same as the space of general solutions to the piezoelectric beam problem. Such an element is said to be superconvergent [29]. Here, one considers this type of approximation.

Assuming that A_{ij} are constant and integrating the equilibrium equations in Eq. (18) for the homogenous case (i.e., $q_x = q_y = 0$), after have condensed out the variables $\bar{\phi}_1$ and $\bar{\phi}_3$, one obtains

$$\bar{A}_{11}u' + \bar{A}_{12}\beta' = c_1 \qquad A_{33}(v' + \beta) = c_2 \qquad \bar{A}_{12}u' + \bar{A}_{22}\beta' = c_3 + c_2 X \tag{19}$$

which exact solution is

$$\begin{Bmatrix} u(X) \\ v(X) \\ \beta(X) \end{Bmatrix} = \frac{1}{\Delta}\begin{bmatrix} \bar{A}_{22}X & -\frac{\bar{A}_{12}}{2}X^2 & -\bar{A}_{12}X & \Delta & 0 & 0 \\ \frac{\bar{A}_{12}}{2}X^2 & \frac{\Delta}{A_{33}}X - \frac{\bar{A}_{11}}{6}X^3 & -\frac{\bar{A}_{11}}{2}X^2 & 0 & -\Delta X & \Delta \\ -\bar{A}_{12}X & \frac{\bar{A}_{11}}{2}X^2 & \bar{A}_{11}X & 0 & \Delta & 0 \end{bmatrix}\begin{Bmatrix} c_1 \\ c_2 \\ c_3 \\ c_4 \\ c_5 \\ c_6 \end{Bmatrix} \tag{20}$$

where c_1 through c_6 are constants of integration, and

$$\Delta = \bar{A}_{11}\bar{A}_{22} - \bar{A}_{12}^2 \qquad \bar{A}_{ij} = A_{ij} - C_1\frac{A_{i4}A_{j4}}{A_{44}} - C_3\frac{A_{i5}A_{j5}}{A_{55}}. \tag{21}$$

To develop the superconvergent model, first one defines the nodal degrees of freedom

$$u_1 = u(0) \qquad v_1 = v(0) \qquad \theta_1 = -\beta(0) \qquad u_2 = u(L_e) \qquad v_2 = v(L_e) \qquad \theta_2 = -\beta(L_e), \tag{22}$$

and then express them in terms of the constants c_i using Eq. (21) to write

$$\mathbf{d} = \frac{1}{\Delta}\begin{bmatrix} 0 & 0 & 0 & \Delta & 0 & 0 \\ 0 & 0 & 0 & 0 & 0 & \Delta \\ 0 & 0 & 0 & 0 & -\Delta & 0 \\ \bar{A}_{22}L_e & -\frac{\bar{A}_{12}L_e^2}{2} & -\bar{A}_{12}L_e & \Delta & 0 & 0 \\ \frac{\bar{A}_{12}L_e^2}{2} & \frac{\Delta L_e}{A_{33}}\left(1 - \frac{2}{\Omega}\right) & -\frac{\bar{A}_{11}L_e^2}{2} & 0 & -\Delta L_e & \Delta \\ \bar{A}_{12}L_e & -\frac{\bar{A}_{11}L_e^2}{2} & -\bar{A}_{11}L_e & 0 & -\Delta & 0 \end{bmatrix}\mathbf{c} \qquad \Omega = \frac{12\Delta}{A_{33}\bar{A}_{11}L_e^2} \tag{23}$$

with

$$\mathbf{d} = \lfloor u_1 \quad v_1 \quad \theta_1 \quad u_2 \quad v_2 \quad \theta_2 \rfloor^T \qquad \mathbf{c} = \lfloor c_1 \quad c_2 \quad c_3 \quad c_4 \quad c_5 \quad c_6 \rfloor^T. \tag{24}$$

Next, one identifies the finite element interpolation functions using Eq. (20) and the inverse relation of Eq. (23):

$$u(X) = \frac{1}{1+\Omega}\mathbf{N}_u^T(X)\mathbf{d} \qquad v(X) = \frac{1}{1+\Omega}\mathbf{N}_v^T(X)\mathbf{d} \qquad \beta(X) = -\frac{1}{1+\Omega}\mathbf{N}_\beta^T(X)\mathbf{d} \tag{25}$$

where

$$\mathbf{N}_u = \begin{Bmatrix} (1+\Omega)\psi_1 \\ -\frac{6\bar{A}_{12}}{\bar{A}_{11}L_e}\psi_1\psi_2 \\ -\frac{3\bar{A}_{12}}{\bar{A}_{11}}\psi_1\psi_2 \\ (1+\Omega)\psi_2 \\ \frac{6\bar{A}_{12}}{\bar{A}_{11}L_e}\psi_1\psi_2 \\ -\frac{3\bar{A}_{12}}{\bar{A}_{11}}\psi_1\psi_2 \end{Bmatrix} \qquad \mathbf{N}_v = \begin{Bmatrix} 0 \\ (\Omega + \psi_1 + 2\psi_1\psi_2)\psi_1 \\ L_e\left(\frac{\Omega}{2} + \psi_1\right)\psi_1\psi_2 \\ 0 \\ (\Omega + \psi_2 + 2\psi_1\psi_2)\psi_2 \\ -L_e\left(\frac{\Omega}{2} + \psi_2\right)\psi_1\psi_2 \end{Bmatrix} \qquad \mathbf{N}_\beta = \begin{Bmatrix} 0 \\ -\frac{6}{L_e}\psi_1\psi_2 \\ (\Omega - 2 + 3\psi_1)\psi_1 \\ 0 \\ \frac{6}{L_e}\psi_1\psi_2 \\ (\Omega - 2 + 3\psi_2)\psi_2 \end{Bmatrix} \tag{26}$$

with $\psi_1 = 1 - X/L_e$ and $\psi_2 = X/L_e$.

Note that such interpolation functions are interdependent and depend on the material properties. This dependency is entirely left in charge of Ω when the host beam and attached piezoelectric layers form a symmetric cross-section because $\bar{A}_{12} = 0$. In this case, the developed flexural interpolation functions $\mathbf{N}_v$ and $\mathbf{N}_\beta$ reduce to that of interdependent interpolation element (IIE) proposed by Reddy [6, 29]. If the parameter Ω is null, i.e. the shear rigidity A_{33} is infinity, relations Eq. (25) degenerate to those of the Euler-Bernoulli element.

The virtual displacements statement associated with Eq. (19) reads

$$-\int_0^{L_e}[(\bar{A}_{11}u' + \bar{A}_{12}\beta')\delta u' + A_{33}(v' + \beta)\delta(v' + \beta) + (\bar{A}_{12}u' + \bar{A}_{22}\beta')\delta\beta']dX$$

$$+\int_0^{L_e}\left(q_x\delta u + q_y\delta v - \phi_u\delta u' - \phi_\beta\delta\beta'\right)dX + \sum_{i=1}^{2}\left(F_{xi}\delta u_i + F_{yi}\delta v_i + M_{zi}\delta\theta_i\right) = 0. \tag{27}$$

Substitution of Eq. (25) into Eq. (27) gives

$$\delta\mathbf{d}^T(-\mathbf{f} + \mathbf{p} + \mathbf{r}) = 0 \tag{28}$$

where

$$\mathbf{f} = \int_0^{L_e}\left[\mathbf{N}_u'\left(\bar{A}_{11}\mathbf{N}_u'^T + \bar{A}_{12}\mathbf{N}_\beta'^T\right) + A_{33}\left(\mathbf{N}_v' + \mathbf{N}_\beta\right)\left(\mathbf{N}_v'^T + \mathbf{N}_\beta^T\right) + \mathbf{N}_\beta'(\bar{A}_{12}\mathbf{N}_u'^T + \bar{A}_{22}\mathbf{N}_\beta'^T)\right]dX\,\mathbf{d} = \mathbf{k}\mathbf{d}$$

$$\mathbf{p} = \int_0^{L_e}\left(q_x\mathbf{N}_u + q_y\mathbf{N}_v - \phi_u\mathbf{N}_u' - \phi_\beta\mathbf{N}_\beta'\right)dX \tag{29}$$

$$\mathbf{r} = \lfloor F_{x1} \quad F_{y1} \quad M_{z1} \quad F_{x2} \quad F_{y2} \quad M_{z2}\rfloor^T$$

In the previous relations observe that: (a) external load vector $\mathbf{p}$ is work equivalent to the distributed forces q_x and q_y, and the voltages $\bar{\phi}_1$ and $\bar{\phi}_3$ applied to the piezoelectric actuator layers; (b) unknown reactions are collected in $\mathbf{r}$.

As Eq. (28) must hold for arbitrary $\delta\mathbf{d}$, the term in parentheses must vanhish to result in the linear system

$$\mathbf{f} = \mathbf{k}\mathbf{d} = \mathbf{p} + \mathbf{r}. \tag{30}$$

The explicit form of the element stiffness matrix $\mathbf{k}$ and of the external load vector $\mathbf{p}$ for uniformly distributed loads $q_x = \bar{q}_x$ and $q_y = \bar{q}_y$ are written, in local coordinates, as

$$\mathbf{k} = \frac{1}{L_e}\begin{bmatrix} \bar{A}_{11} & 0 & -\bar{A}_{12} & -\bar{A}_{11} & 0 & \bar{A}_{12} \\ & \frac{4}{L_e^2}\omega & \frac{2}{L_e}\omega & 0 & -\frac{4}{L_e^2}\omega & \frac{2}{L_e}\omega \\ & & \omega + \bar{A}_{22} & \bar{A}_{12} & -\frac{2}{L_e}\omega & \omega - \bar{A}_{22} \\ & & & \bar{A}_{11} & 0 & -\bar{A}_{12} \\ & \text{sym.} & & & \frac{4}{L_e^2}\omega & -\frac{2}{L_e}\omega \\ & & & & & \omega + \bar{A}_{22} \end{bmatrix} \qquad \omega = \frac{1}{1+\Omega}\frac{3\Delta}{\bar{A}_{11}} \tag{31}$$

$$\mathbf{p} = \frac{1}{1+\Omega}\frac{\bar{q}_x L_e}{2}\begin{Bmatrix} 1+\Omega \\ -2\bar{A}_{12}/L_e\bar{A}_{11} \\ -\bar{A}_{12}/\bar{A}_{11} \\ 1+\Omega \\ 2\bar{A}_{12}/L_e\bar{A}_{11} \\ -\bar{A}_{12}/\bar{A}_{11} \end{Bmatrix} + \frac{\bar{q}_y L_e}{2}\begin{Bmatrix} 0 \\ 1 \\ L_e/6 \\ 0 \\ 1 \\ -L_e/6 \end{Bmatrix} + \phi_u\begin{Bmatrix} 1 \\ 0 \\ 0 \\ -1 \\ 0 \\ 0 \end{Bmatrix} + \phi_\beta\begin{Bmatrix} 0 \\ 0 \\ -1 \\ 0 \\ 0 \\ 1 \end{Bmatrix}.$$

The linear system Eq. (30) of each element must be written first in the global system $X_g Y_g$ to then obtain the assembled linear system of the entire structure from all element contributions. In the notation of Fig. 4, the displacements $\mathbf{d}$ and forces $\mathbf{f}$ in the local system XY are related to the displacements $\mathbf{d}_g$ and forces $\mathbf{f}_g$ in the global system $X_g Y_g$ by means of

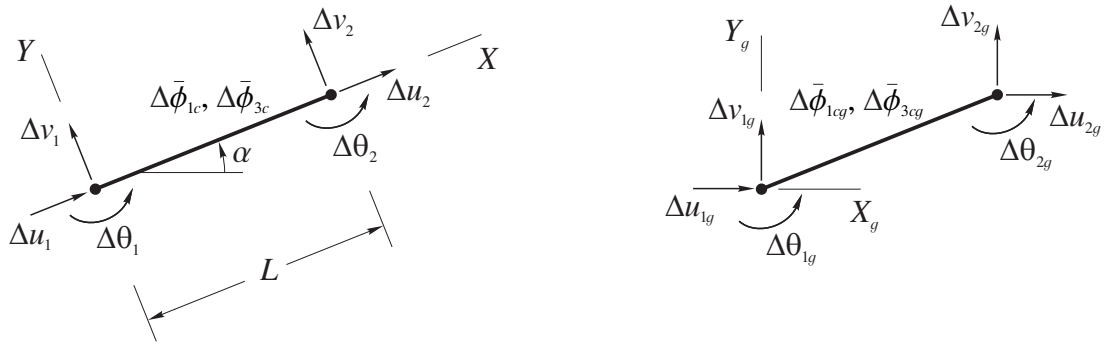

Local system Global system

Figure 4. (a) Components of $\mathbf{d}$ in the local system XY; (b) components of $\mathbf{d}_g$ in the global system X_gY_g

$$\mathbf{d} = \mathbf{T}\mathbf{d}_g \qquad \mathbf{f} = \mathbf{T}\mathbf{f}_g \qquad \mathbf{T} = \begin{bmatrix} \cos\alpha & \sin\alpha & 0 & 0 & 0 & 0 \\ -\sin\alpha & \cos\alpha & 0 & 0 & 0 & 0 \\ 0 & 0 & 1 & 0 & 0 & 0 \\ 0 & 0 & 0 & \cos\alpha & \sin\alpha & 0 \\ 0 & 0 & 0 & -\sin\alpha & \cos\alpha & 0 \\ 0 & 0 & 0 & 0 & 0 & 1 \end{bmatrix} \tag{32}$$

where the fact that $\mathbf{T}$ is orthogonal implies that the element tangent stiffness matrix in both systems are related by

$$\mathbf{k}_g = \mathbf{T}^T\mathbf{k}\mathbf{T}. \tag{33}$$

Because the magnitudes of the coefficients C_{ij}, e_{ij} and ξ_i are quite different, the condition number of the global stiffness matrix can be very high. To overcome this problem, the simple and effective procedure proposed by Qi et al. [30] is adopted.

This element gives exact values of u, v and β at the nodes independent of the load distribution because the finite element approximation space is the same as the space of general solutions to the associated Timoshenko beam problem, and all distributed loads are properly represented as nodal loads. Such a procedure results in an efficient and accurate locking-free finite element for the analysis of frame structures according to the Timoshenko as well as classical beam theories. The element may be adapted to include other features such as the geometric [31] and material nonlinearities.

Note that although the interpolation functions $\mathbf{N}_u$, $\mathbf{N}_v$, $\mathbf{N}_\beta$ yields exact nodal values for the mechanical variables, they do not bring any information about the accuracy of the condensed variables $\bar{\phi}_1$ and $\bar{\phi}_3$ which are in turn defined by the first derivatives of $\mathbf{N}_v$ and $\mathbf{N}_\beta$. The fundamental question then arises: do such variables also possess nodal superconvergence? In what follows one gives vision and insight in answering this question.

From the constitutive relations Eq. (14),

$$\begin{Bmatrix} N \\ M \end{Bmatrix} = \begin{bmatrix} A_{11} & A_{12} \\ A_{12} & A_{22} \end{bmatrix} \begin{Bmatrix} u' \\ \beta' \end{Bmatrix} + \begin{bmatrix} A_{14} & A_{15} \\ A_{24} & A_{25} \end{bmatrix} \begin{Bmatrix} \bar{\phi}_1 \\ \bar{\phi}_3 \end{Bmatrix} = \mathbf{a}_\sigma \begin{Bmatrix} u' \\ \beta' \end{Bmatrix} + \mathbf{a}_{\sigma\xi} \begin{Bmatrix} \bar{\phi}_1 \\ \bar{\phi}_3 \end{Bmatrix}$$

$$\begin{Bmatrix} 0 \\ 0 \end{Bmatrix} = \begin{bmatrix} A_{14} & A_{24} \\ A_{15} & A_{25} \end{bmatrix} \begin{Bmatrix} u' \\ \beta' \end{Bmatrix} + \begin{bmatrix} A_{44} & 0 \\ 0 & A_{55} \end{bmatrix} \begin{Bmatrix} \bar{\phi}_1 \\ \bar{\phi}_3 \end{Bmatrix} = \mathbf{a}_{\sigma\xi}^T \begin{Bmatrix} u' \\ \beta' \end{Bmatrix} + \mathbf{a}_\xi \begin{Bmatrix} \bar{\phi}_1 \\ \bar{\phi}_3 \end{Bmatrix} \tag{34}$$

which implies that

$$\mathbf{a}_\sigma^{-1} \begin{Bmatrix} N \\ M \end{Bmatrix} = \begin{Bmatrix} u' \\ \beta' \end{Bmatrix} + \mathbf{a}_\sigma^{-1}\mathbf{a}_{\sigma\xi} \begin{Bmatrix} \bar{\phi}_1 \\ \bar{\phi}_3 \end{Bmatrix} \qquad \mathbf{a}_{\sigma\xi}^T \begin{Bmatrix} u' \\ \beta' \end{Bmatrix} = -\mathbf{a}_\xi \begin{Bmatrix} \bar{\phi}_1 \\ \bar{\phi}_3 \end{Bmatrix} \tag{35}$$

where $\mathbf{a}_\sigma$and $\mathbf{a}_\xi$ are positive and negative definite matrices, and $\mathbf{a}_{\sigma\xi}$ is singular if some of the outer layers do not exhibit piezoelectricity. Substitution of the last equation of Eq. (35) into the former equation pre-multiplied by $\mathbf{a}_{\sigma\xi}^T$ gives

Table 1. Properties of PZT-5H

GPa					$\mathrm{C/m^2}$			$\mathrm{nC^2/Nm^2}$	
C_{11}	C_{12}	C_{13}	C_{33}	C_{44}	e_{31}	e_{33}	e_{15}	ξ_1	ξ_3
126	79.5	84.1	117	23	-6.5	23.3	17	15.05	13.02

$$\begin{Bmatrix} \bar{\phi}_1 \\ \bar{\phi}_3 \end{Bmatrix} = \mathbf{b} \begin{Bmatrix} N \\ M \end{Bmatrix} \qquad \mathbf{b} = \left(\mathbf{a}_{\sigma\xi}^T \mathbf{a}_\sigma^{-1} \mathbf{a}_{\sigma\xi} - \mathbf{a}_\xi\right)^{-1} \mathbf{a}_{\sigma\xi}^T \mathbf{a}_\sigma^{-1}. \tag{36}$$

Evaluation of Eq. (36) at the nodes, taking into account the boundary conditions Eq. (10), result in

$$\begin{Bmatrix} \bar{\phi}_1(0) \\ \bar{\phi}_3(0) \\ \bar{\phi}_1(L_e) \\ \bar{\phi}_3(L_e) \end{Bmatrix} = \mathbf{BLr} \qquad \mathbf{B} = \begin{bmatrix} \mathbf{b} & \mathbf{0} \\ \mathbf{0} & \mathbf{b} \end{bmatrix} \qquad \mathbf{L} = \begin{bmatrix} -1 & 0 & 0 & 0 & 0 & 0 \\ 0 & 0 & 1 & 0 & 0 & 0 \\ 0 & 0 & 0 & 1 & 0 & 0 \\ 0 & 0 & 0 & 0 & 0 & -1 \end{bmatrix}. \tag{37}$$

According to the Betti's theorem, the nodal reactions $\mathbf{r}$ are exact with respect to the element formulation regardless the loading pattern if the nodal displacements are calculated accordingly. Since the right-hand-side of Eq. (37) presents nodal superconvergence, the same is expected for the left-hand-side of the equation so that the electrical variables $\bar{\phi}_1$ and $\bar{\phi}_3$ are anticipated to be exactly evaluated at the nodes. In what follows, this hypothesis is numerically tested.

4 Numerical examples

According to the mathematical model, the piezoelectric layers solely operate in extension mode since both polarization and electric field are in the Y- direction. In the numerical evaluation of the constitutive parameters $\tilde{Q}_{11}$, $\tilde{e}_{31}$ and $\tilde{\xi}_3$ in Eq. (12) , the host structure is assumed to be made of aluminum with Young´s modulus $E = 70.3$ GPa and Poisson´s ratio $\nu = 0.345$, and the piezoelectric layers are assumed to be made of PZT-5H with properties indicated in Table 1 [32]. As a transversely isotropic material (isotropic in the plane normal to Y-axis), the PZT-5H presents $C_{23} = C_{13}$, $C_{22} = C_{11}$, $C_{55} = C_{44}$, $C_{66} = (C_{11} - C_{12})/2$, $e_{32} = e_{31}$, $e_{24} = e_{15}$ and $\xi_2 = \xi_1$. The accuracy and effectiveness of the proposed element under mechanical loading is demonstrated by means of two linear static problems adopting the following geometry (units in mm): $b = b_1 = b_3 = 25$, $2h = 2$ and $t_1 = t_3 = 1$. A code in MATLAB language has been written to carry out the numerical tests. It is interesting note that all numerical pitfalls due to the huge difference magnitude order involving the mechanic and piezoelectric dielectric constants [30, 33] are absent in the proposed formulation, because only mechanical degrees of freedom are concerned with the solution.

4.1 Simply supported beam with distributed axial load and sensing

A simply supported beam is subjected to the distributed axial load $\bar{q}_x = \bar{q}$ ($\bar{q}_y = 0$), with two symmetrical piezoelectric layers ($C_1 = C_3 = 1$) continuously distributed as sensors. The simply supported boundary conditions $u(0) = v(0) = M(0) = 0$ and $N(L) = v(L) = M(L) = 0$ applied to the governing equations Eq. (9) yield the following closed form solutions for the displacements and rotation components, and for the sensed electric potentials:

$$\begin{aligned} u(X) &= \bar{q}L^2 \frac{\bar{A}_{22}}{\Delta}\left(1 - \frac{1}{2}\frac{X}{L}\right)\frac{X}{L} \\ v(X) &= -\frac{\bar{q}L^3}{3}\frac{\bar{A}_{12}}{\Delta}\left(1 - \frac{3}{2}\frac{X}{L} + \frac{1}{2}\frac{X^2}{L^2}\right)\frac{X}{L} \\ \beta(X) &= \frac{\bar{q}L^2}{3}\frac{\bar{A}_{12}}{\Delta}\left(1 - 3\frac{X}{L} + \frac{3}{2}\frac{X^2}{L^2}\right) \end{aligned} \tag{38}$$

Table 2. Finite element solutions of a simply supported beam under uniformly distributed axial load

L/H	mesh	$u(\bar{X})$	$v(\bar{X})$	$\beta(\bar{X})$	$\bar{\phi}_1(\bar{X})$	$\bar{\phi}_3(\bar{X})$
	1	7.953845E-12	0.	0.	-1.085065E-03	-1.085065E-03
4	2	1.363516E-11	0.	0.	-7.233765E-04	-7.233765E-04
	3	1.704395E-11	0.	0.	-3.616883E-04	-3.616883E-04
	1	7.953845E-08	0.	0.	-1.085065E-01	-1.085065E-01
400	2	1.363516E-07	0.	0.	-7.233765E-02	-7.233765E-02
	3	1.704395E-07	0.	0.	-3.616883E-02	-3.616883E-02

and

$$\bar{\phi}_1(X) = \bar{q}L\frac{\Delta_1}{\Delta}\left(1-\frac{X}{L}\right) \qquad \bar{\phi}_3(X) = \bar{q}L\frac{\Delta_3}{\Delta}\left(1-\frac{X}{L}\right) \tag{39}$$

where

$$\Delta_1 = \frac{A_{24}\bar{A}_{12} - A_{14}\bar{A}_{22}}{A_{44}} \qquad \Delta_3 = \frac{A_{25}\bar{A}_{12} - A_{15}\bar{A}_{22}}{A_{55}}. \tag{40}$$

Taking $\bar{q} = 1$ and coarse meshes of just two elements, Table 2 shows the finite element solutions evaluated at $X = \bar{X}$ (single domain node position) making $\bar{X} = L/4$, $\bar{X} = L/2$ and $\bar{X} = 3L/4$ for the meshes 1, 2 and 3, respectively. The table results are obtained using $L/H = 4$ and $L/H = 400$, where $H = 2h + t_1 + t_2$. According to the developed procedure note that: (a) no shear locking takes place, (b) computed nodal values are exact with respect to the formulation due to the superconvergent feature embodied in the element interpolation functions, and (c) few elements are adequate to precisely capture the static response for both mechanical and electrical variables.

4.2 Simply supported beam with distributed transverse load and sensing

With respect to the previous example, the following change is carried out: the applied distributed axial load is replaced by the distributed transverse load $\bar{q}_y = \bar{q}$ ($\bar{q}_x = 0$). The simply supported boundary conditions $u(0) = v(0) = M(0) = 0$ and $N(L) = v(L) = M(L) = 0$ applied to the governing equations Eq. (9) yield the following closed form solutions for the displacements and rotation components, and for the sensed electric potentials:

$$\begin{aligned} u(X) &= -\frac{\bar{q}L^3}{4}\frac{\bar{A}_{12}}{\Delta}\left(1-\frac{2}{3}\frac{X}{L}\right)\frac{X^2}{L^2} \\ v(X) &= \frac{\bar{q}L^4}{24}\frac{\bar{A}_{11}}{\Delta}\left(1-2\frac{X^2}{L^2}+\frac{X^3}{L^3}\right)\frac{X}{L} + \frac{\bar{q}L^2}{2A_{33}}\left(1-\frac{X}{L}\right)\frac{X}{L} \\ \beta(X) &= -\frac{\bar{q}L^3}{24}\frac{\bar{A}_{11}}{\Delta}\left(1-6\frac{X^2}{L^2}+4\frac{X^3}{L^3}\right) \end{aligned} \tag{41}$$

and

$$\bar{\phi}_1(X) = \frac{\bar{q}L^2}{2}\frac{\Delta_2}{\Delta}\left(1-\frac{X}{L}\right)\frac{X}{L} \qquad \bar{\phi}_3(X) = \frac{\bar{q}L^2}{2}\frac{\Delta_4}{\Delta}\left(1-\frac{X}{L}\right)\frac{X}{L} \tag{42}$$

where

$$\Delta_2 = \frac{A_{14}\bar{A}_{12} - A_{24}\bar{A}_{11}}{A_{44}} \qquad \Delta_4 = \frac{A_{15}\bar{A}_{12} - A_{25}\bar{A}_{11}}{A_{55}}. \tag{43}$$

Table 3. Finite element solutions of a simply supported beam under uniformly distributed transverse load

L/H	mesh	$u(\bar{X})$	$v(\bar{X})$	$\beta(\bar{X})$	$\bar{\phi}_1(\bar{X})$	$\bar{\phi}_3(\bar{X})$
	1	0.	7.671948E-11	1.254316E-08	-2.450042E-03	2.450042E-03
4	2	0.	1.068538E-10	0.	-3.266722E-03	3.266722E-03
	3	0.	7.671948E-11	-1.254316E-08	-2.450042E-03	2.450042E-03
	1	0.	6.499757E-03	1.254316E-02	-2.450042E+01	2.450042E+01
400	2	0.	9.122457E-03	0.	-3.266722E+01	3.266722E+01
	3	0.	6.499757E-03	-1.254316E-02	-2.450042E+01	2.450042E+01

Taking $\bar{q} = 1$ and coarse meshes of a pair of elements, Table 3 shows the finite element solutions evaluated at $X = \bar{X}$ (single domain node position) making $\bar{X} = L/4$, $\bar{X} = L/2$ and $\bar{X} = 3L/4$ for the meshes 1, 2 and 3, respectively. Note again that the displacements, rotation and sensed electric potentials are exactly evaluated.

5 Conclusions

The superconvergent beam finite element for piezoelectric plane frames has its efficiency proven by numerical examples. The element equations are analytically and consistently formulated. The superconvergent linear element developed: (a) has interpolation functions dependent on the mechanical properties of the materials and the electrical properties of the sensor layers, (b) has the same degrees of freedom as its purely mechanical counterpart; (c) does not suffer from shear locking; (d) exhibits no numerical pitfalls associated with the huge difference between the magnitude order of the mechanic and dielectric constants; (e) computes exact nodal values with respect to the Timoshenko assumption regardless the applied loading pattern.

The superconvergent feature embodied in the interpolation functions make this element ideally suited for frame structural analysis because few elements per a structural member still yields exact nodal results. It is hoped that the understanding and insight gained through that beam finite element model, one may be able to develop simple but reliable shear deformable plate elements.

Authorship statement. The authors hereby confirm that they are the sole liable persons responsible for the authorship of this work, and that all material that has been herein included as part of the present paper is either the property (and authorship) of the authors, or has the permission of the owners to be included here.

References

[1] D. J. Leo. *Engineering Analysis of Smart Material Systems*. John Wiley, 2007.
[2] D. Marinković and Z. Marinković, "On FEM modeling of piezoelectric actuators and sensors for thin-walled structures". *Smart Structures and Systems*, vol. 9, n. 5, pp. 411–426, 2012.
[3] I. M. Bendary, M. A. Elshafei and A. M. Riad, "Finite element model of smart beams with distributed piezoelectric actuators". *Journal of Intelligent Material Systems and Structures*, vol. 21, n. 7, pp. 747–758, 2010.
[4] K. R. Kumar and S. Narayanan, "Active vibration control of beams with optimal placement of piezoelectric sensor/actuator pairs". *Smart Materials and Structures*, vol. 17, n. 5, pp. 55008–55022, 2008.
[5] L. N. Sulbhewar and P. Ravenndranath, "A numerically accurate and efficient coupled polynomial field interpolation for Euler-Bernoulli piezoelectric beam finite element with induced potential effect", *Journal of Intelligent Material Systems and Structures*, vol. 26, n. 12, pp.1539–1550, 2014.
[6] J. N. Reddy, "On locking-free shear deformable beam finite elements". *Computer Methods in Applied Mechanics and Engineering*, vol. 149, n. 1–4, pp. 113–132, 1997.
[7] D. H. Robbins and J. N. Reddy, "Analysis of piezoelectrically actuated beams using a layer-wise displacement theory". *Computers and Structures*, vol. 41, n. 2, pp. 265–279, 1991.
[8] M. H. H. Shen, "A new modeling technique for piezoelectrically actuated beams". *Computers and Structures*, vol. 57, n. 3, pp. 361–366, 1995.

[9] S. Narayanan and V. Balamurugan, "Finite element modelling of piezolaminated smart structures for active vibration control with distributed sensors and actuators". *Journal of Sound and Vibration*, vol. 262, n. 3, pp. 529–562, 2003.
[10] M. C. Ray and N. Mallik, "Active control of laminated composite beams using a piezoelectric fiber reinforced composite layer". *Smart Materials and Structures*, vol. 13, n. 1, pp. 146–152, 2004.
[11] M. A. Neto, W. Yu and S. Roy, "Two finite elements for general composite beams with piezoelectric actuators and sensors". *Finite Elements in Analysis and Design*, vol. 45, n. 5, pp. 295–304, 2009.
[12] M. Křiek, "Superconvergence phenomena in the finite element method". *Computer Methods in Applied Mechanics and Engineering*, vol. 116, n. 1-4, pp. 157–163, 1994.
[13] J. J. Douglas and T. Dupont, "Superconvergence for Galerkin methods for the two-point boundary problem via local projections", *Numerische Mathematik*, vol. 21, n. 3, pp. 270–278, 1973.
[14] J. N. Reddy. *Energy Principles and Variational Methods in Applied Mechanics*. John Wiley, 2002.
[15] R. Lammering, "The application of a finite shell element for composites containing piezo-electric polymers in vibration control". *Computers and Structures*, vol. 41, n. 5, pp. 1101–1109, 1991.
[16] A. Almajid, M. Taya and S. Hudnut, "Analysis of out-of-plane displacement and stress field in a piezocomposite plate with functionally graded microstructure". *International Journal of Solids Structures*, vol. 38, n. 19, pp. 3377–3391, 2001.
[17] M. A. Trindade, A. Benjeddou and R. Ohayon, "Finite element modelling of hybrid active-passive vibration damping of multilayer piezoelectric sandwich beams – Part I: formulation". *International Journal for Numerical Methods in Engineering*, vol. 51, n. 7, pp. 835–854, 2001.
[18] K. Y. Sze, X. M. Yang and H. Fan, "Electric assumptions for piezoelectric laminate analysis". *International Journal of Solids Structures*, vol. 41, n. 9-10, pp. 2363–2382, 2004.
[19] D. Marinković, H. Köppe and U. Gabbert, "Aspects of modeling piezoelectric active thin-walled structures". *Journal of Intelligent Material Systems and Structures*, vol. 20, n. 15, pp. 1835–1844, 2009.
[20] A. L. Carvalho Neto, R. R. F. Santos, E. Lucena Neto and F. A. C. Monteiro, "Piezoelectric beams under small strains but large displacements and rotations". *Applied Mathematical Modelling*, vol. 87, pp. 430–445, 2020.
[21] I. M. Gelfand and S. V. Fomin. *Calculus of Variations*. Dover, 2000.
[22] J. R. Hutchinson, "Shear coefficients for Timoshenko beam theory". *Journal of Applied Mechanics*, vol. 68, n. 1, pp. 87–92, 2001.
[23] S. Puchegger, S. Bauer, D. Loidl, K. Kromp and H. Peterlik, "Experimental validation of the shear correction factor". *Journal of Sound and Vibration*, vol. 261, n. 1, pp. 177–184, 2003.
[24] A. Butz, S. Klinkel and W. Wagner, "A geometrically and materially non-linear piezoelectric three-dimensional-beam finite element formulation including warping effects". *International Journal for Numerical Methods in Engineering*, vol. 76, n. 5, pp. 601–635, 2008.
[25] A. A. Khdeir, E. Darraj and O. J. Aldraihem, "Free vibration of cross ply laminated beams with multiple distributed piezoelectric actuators". Journal of Mechanics, vol. 28, n. 1, pp. 217–227, 2012.
[26] M. A. Elshafei, M. R. Ajala and A. M. Riad, "Modeling and analysis of smart Timoshenko beams with piezoelectric materials". *International Journal of Engineering and Innovative Technology*, vol. 3, n. 11, pp. 21–33, 2014.
[27] L.N. Sulbhewar and P. Raveendranath, "An accurate novel coupled field Timoshenko piezoelectric beam finite element with induced potential effects". *Latin American Journal of Solids and Structures*, vol. 11, n. 9, pp. 1628–1650, 2014.
[28] J. Yang. *An Introduction to the Theory of Piezoelectricity*. Springer, 2018.
[29] J. N. Reddy. *An Introduction to the Finite Element Method*. McGraw-Hill, 2006.
[30] H. Qi, D. Fang and Z. Yao, "FEM analysis of electro-mechanical coupling effects of piezoelectric materials", *Computational Materials Science*, vol. 8, n. 4, pp. 283–290, 1997.
[31] J. G. S. A. Meireles, R. P. Barros, E. Lucena Neto and F. A. C. Monteiro, "An efficient locking free corotational beam finite element". In: *Proceedings of the XL Ibero-Latin American Congress on Computational Methods in Engineering (XL CILAMCE)*.
[32] J. Yang. *An Introduction to the Theory of Piezoelectricity*. Springer, 2018.
[33] E. L. Cardoso and J. S. Fonseca, "An incremental Lagrangian formulation to the analysis of piezo-electric bodies subjected to geometric non-linearities". *International Journal for Numerical Methods in Engineering*, vol. 59, n. 7, pp. 963–987, 2004.